IOWA STATE UNIVERSITY
Digital Repository

Graduate Theses and Dissertations

Iowa State University Capstones, Theses and Dissertations

2010

Photovoltaic activity in benzobisoxazole based conjugated polymers

Molly Reida
Iowa State University

Follow this and additional works at: https://lib.dr.iastate.edu/etd

 Part of the Electrical and Computer Engineering Commons

Recommended Citation
Reida, Molly, "Photovoltaic activity in benzobisoxazole based conjugated polymers" (2010). *Graduate Theses and Dissertations*. 11476.
https://lib.dr.iastate.edu/etd/11476

This Thesis is brought to you for free and open access by the Iowa State University Capstones, Theses and Dissertations at Iowa State University Digital Repository. It has been accepted for inclusion in Graduate Theses and Dissertations by an authorized administrator of Iowa State University Digital Repository. For more information, please contact digirep@iastate.edu.

www.manaraa.com

Photovoltaic activity in benzobisoxazole based conjugated polymers

by

Molly Reida

A thesis submitted to the graduate faculty

in partial fulfillment of the requirements for the degree of

MASTER OF SCIENCE

Major: Electrical Engineering

Program of Study Committee:
Sumit Chaudhary, Major Professor
Liang Dong
Nathan Neihart

Iowa State University

Ames, Iowa

2010

Copyright © Molly Reida, 2010. All right reserved.

www.manaraa.com

Table of Contents

www.manaraa.com

www.manaraa.com

Abstract

The material and photovoltaic properties of a new class of conjugated polymers was investigated. These two new polymers; poly (3,4-didodecylthiopene vinylene)-2,6-diyl benzo [1,2-d; 5,4-d'] bisoxazole] (cis-DD-PTVBBO) and poly (3,4-didodecylthiopene vinylene)-2,6-diyl benzo [1,2-d; 4,5-d'] bisoxazole] (trans-DD-PTVBBO) were synthesized by Malika Jeffries-El group (Department of Chemistry, Iowa State University). Electron affinities were measured be 3.02eV for cis-DD-PTVBBO and 3.10eV for trans-DD-PTVBBO. The optical bandgaps are around 2eV for both polymers.

The low band gap and high electron affinity of these polymers suggest that they would be suitable candidates for use in bulk heterojunction solar cells with Phyenyl-C61-butyric acid methyl ester (PCBM). Solar cells using the cis-DD-PTVBBO and the trans-DD-PTVBBO as the electron donor were fabricated and device characteristics were measured. In addition, hole mobilities were measured and atomic force microscopy (AFM) characterization was performed to evaluate phase separation in the thin films of the active layers.

Photovoltaic performance was lower than expected and is suspected to be due to poor solubility and large aggregates within the active layer thin film. In addition, it is suspected that poor performance may be due to internal charge transfer between the electron donating thiophene unit and electron accepting benzobisoxazole unit. Having these two units is good in the sense that it delocalizes the charge and reduces the band gap of conjugated polymers; however, it may also lead to reduced electron transfer to the PCBM phase, leading to poor performance of photovoltaic cells.

www.manaraa.com

Chapter 1: Introduction

1.1 Organic solar cells

As the world demand for energy continues to increase, more focus is placed on renewable energy every year. Traditional fossil fuels, although currently the most economical are of a limited supply and are also a contributing factor to environmental health concerns such as global warming and smog. The development of clean and inexpensive alternatives to fossil fuels is an area of much research and growth. In fact, between 2004 and 2008, the annual renewable energy investment had increased fourfold to reach $120 billion while in that same time the increase in photovoltaic (PV) capacity increased sixfold [1].

Solar cells based on organic semiconductors have some attractive properties when compared to traditional crystalline solar cells. Crystalline solar cells require expensive source wafers and high temperature processes, which add to the manufacturing cost. The absorption coefficient of organics is high allowing them to be made from very thin films. Organics also have the ability to be processed in solution allowing them to be easily manufactured through reel-to-reel inkjet printing or spray deposition at low temperatures. The synthesis of organic materials is simple and inexpensive, allowing fine tuning of the material properties. Organics also have the ability to be deposited on ultra thin and flexible materials allowing for the possibility of integration into building materials [2] and even fabrics [3].

Despite these advantages, there are several disadvantages of organic semiconductors as well, including low mobility and low exciton diffusion length. Many organic materials are

www.manaraa.com

sensitive to light and oxygen and must be fabricated in oxygen and/or light free environments before they can be encapsulated. The efficiency of organic based cells is currently lower than its inorganic counterparts, but the development of new materials and processing techniques continue to increase efficiencies and bring them closer to the efficiencies achieved by inorganics at a potentially much lower cost.

1.2 Basic physics

The fundamental mechanism of operation for organic solar cells consists of four basics steps: 1) absorption of light and generation of excitons (electron-hole pairs), 2) diffusion of excitons, 3) dissociation of excitons and generation of charges, and 4) charge transport and collection. The donor-acceptor system governs all aspects of this mechanism except charge collection. Charge collection is based on the electronic interface between the active layer and its corresponding electrode.

Light absorption and the generation of excitons will occur for energies at or above the bandgap of the donor material; therefore, the bandgap of the donor material should be such that it is able to absorb frequencies within the solar spectrum. The solar spectrum peaks around 600nm and the ideal bandgap for absorbing most of the solar spectrum is around 1.4eV.

Upon excitation, the donor must be able to transfer charge to the acceptor. A driving force must be present to ensure that it is energetically favorable for the donor to transfer the charge and this force must be greater than the binding energy of the exciton; generally estimated to be around 0.4-0.5eV [4], although exciton separation has be documented for donor-acceptor offsets as low as 0.3eV [5]. This force can be represented by the difference

www.manaraa.com

between the lowest unoccupied molecular orbitals (LUMOs) of the donor and acceptor. This driving force effects dissociation of the exciton with the formation of a geminate pair. An additional force is needed to separate the geminate pair into free charges. This is aided both thermally and by the intrinsic electric field within the device. Mobilities of around 10^{-4} cm^2/Vs or higher have been shown to be necessary for efficient geminate separation. The electron and hole mobilities must be high enough and/or balanced enough to prevent the build up of space charge, which can reduce the extraction of charge carriers. The mobilities should also be high enough to transport through the device before recombination [5]. The open circuit voltage of organic solar cells is determined by the difference between the highest occupied molecular orbital (HOMO) level of the donor and the LUMO level of the acceptor [4].

Currently the most successful organic photovoltaic (PV) devices produced are based on polymer-fullerene bulk-heterojunction (BHJ) systems. Due to the short lifetime and low mobility of excitons, the diffusion length of excitons in organic semiconductors is generally on the order of 10nm. This imposes the condition that anywhere within the active layer, the distance to the interface should be on the order of the exciton diffusion length. This is done by mixing the electron donor and acceptor materials which naturally phase separate at the nanometer dimension and is referred to as a bulk heterojunction (BHJ) as shown in Figure 1. This allows the surface area of the junctions to be maximized and is irrespective to the overall film thickness [6]. Unfortunately, this also produces dead ends and isolated domains that trap charge carriers and prevent them from being extracted. Replacing the disordered electron acceptor with an ordered nanostructure may be a viable route.

www.manaraa.com

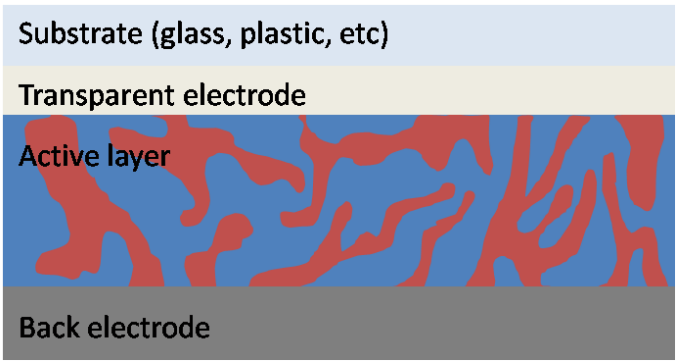

Figure 1: Bulk-heterojunction solar cell architecture.

1.3 History and state of the art

An ideal nanostructure would have small, straight pores and be thick enough to absorb most of the sunlight. The pore radius should be slightly less than the exciton diffusion length to enable maximum exciton harvesting. The pores should be straight to provide a direct path to the anode and cathode [5]. Nanostructured titania (TiO_2) and zinc oxide (ZnO) have both been used as nanostructured electrodes; however with poor power conversion efficiencies of between 0.2-1% [7]. This is due mostly to the imperfect nanostructure of these materials. It is difficult to fabricate nanostructures with pore sizes on the order of 10nm with high aspect ratios [5] and to get the polymer to infiltrate the structure completely; which results in a lower interfacial area between donor and acceptor material than is present in BHJ cells [7]. One strategy is to incorporate an organic or organometallic dye at the polymer/metal oxide interface in order to assist the processes of light harvesting, charge separation, and photocurrent generation [8]. Power conversion efficiencies as high as 3.8% have been reported for solar cells based on a TiO_2 nanotube array vertically oriented from the fluorine doped tin oxide (FTO) coated glass substrate, sensitized with unsymmetrical squaraine dye (SQ-1) that absorbs in the red and near infrared portion of solar

www.manaraa.com

spectrum, and which are uniformly infiltrated with p-type regioregular poly(3-hexylthiophene-2,5-diyl) (P3HT) that absorbs higher energy photons [9]. This structure is shown in Figure 2. Currently bulk-heterojunction cells outperform nanostructured cells.

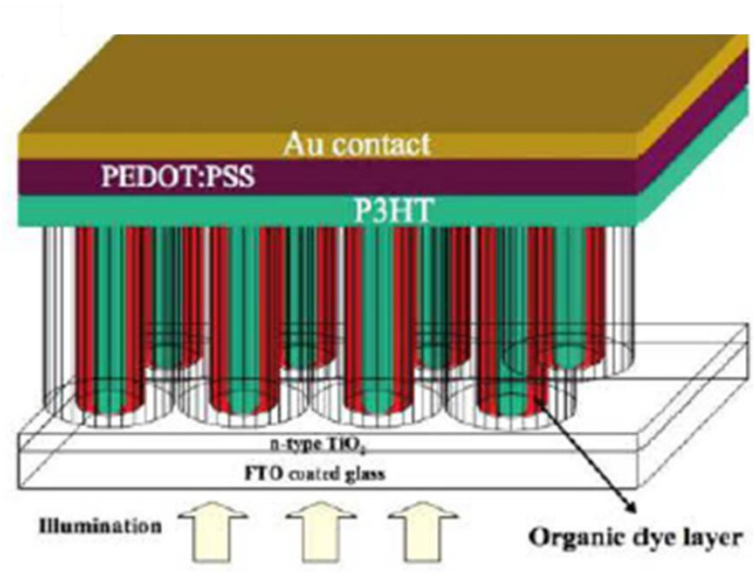

Figure 2: Nanostructured solar cells with power conversion efficiency of 3.8%.

The most widely studied organic photovoltaic system is the poly (3-hexylthiophene) (P3HT), and [6,6]-phenyol-C61-butyric acid methyl ester (PCBM), which has reproducible efficiencies of 5%. P3HT is a derivative of thiophene chains and acts as the donor in BHJ cells. The 3-hexyl substitutes can be substituted into the polymer chain with two different regioregularities; head to head (HH) or head to tail (HT) (Figure 3). Regiorandom P3HT consists of both HH and HT 3-hexylthiophenes, while regioregular consists of only one kind of structure. The type of P3HT used in organic solar cells is regioregular head to tail (Figure 3). PCBM (Figure 4) is a synthesized soluble derivative of the buckminsterfullerene (C_{60}) which can be electrochemically reduced up to six electrons, thus acting as an acceptor in BHJ solar cells.

www.manaraa.com

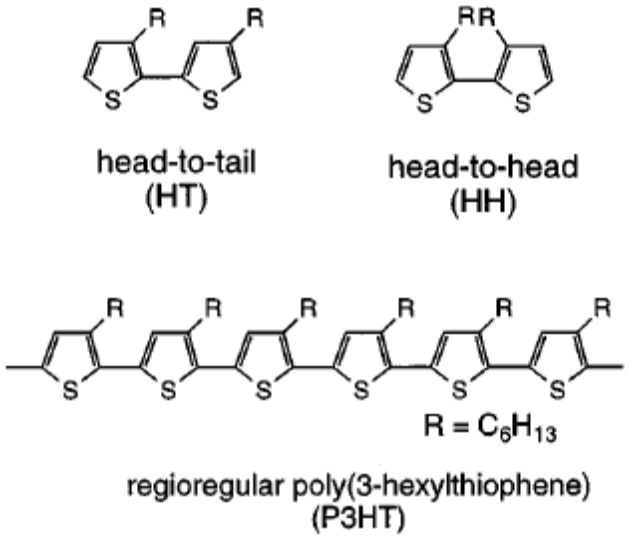

Figure 3: P3HT molecular structure [10].

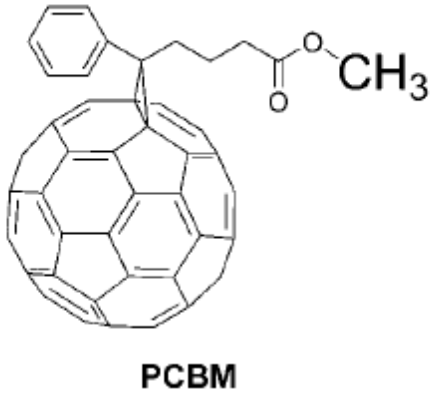

Figure 4: PCBM molecular structure [11].

One of the reasons P3HT has been more successful than other polymers used to date is that it has a relatively high hole mobility, up to $10^{-4}cm^2/Vs$, which balances well with the high electron mobility of PCBM ($2x10^{-3}cm^2/Vs$). Another reason is that the film morphology

www.manaraa.com

has been closely studied and its process parameters have been optimized. In 2002, efficiencies of 2.5% were common with this system [2]. In 2005 an efficiency of 3.85% had been reached [6], and by 2007 the first 5% efficient cells had been fabricated [5]. There are numerous factors to be optimized in the production of organic solar cells including weight ratio and concentration of the two materials, purity of the materials, choice of solvent, spin coating conditions, and annealing conditions, all of which have been shown to have an effect of the film morphology which has a direct correlation to performance. The best weight ratio for P3HT/PCBM cells has been shown to be approximately 1:1, although good devices have been fabricated from weight ratios as low as 1:0.43. It is unclear how much the percent of regioregularity affects device performance. Some authors have shown that a higher percent of regioregularity corresponds to better performance, while others have shown very little difference in device performance. All experiments testing the effect of higher regioregularity have used greater than 90% regioregularity suggesting that although not one of the most important parameters, one would not expect to get the same performance with regiorandam P3HT. The most commonly used solvent is chlorobenzene or variations of, such as dichlorobenzene or ortho-dichlorobenzene. Higher molecular weights correspond to a red shift in the absorption spectrum, a higher absorption coefficient, and higher hole mobilities. Different spin coating conditions will result in different active layer thicknesses. The desired thickness is a function of absorption and; therefore, a function of almost every other parameter. Annealing conditions have been shown to have drastic effects on device performance. There are two different ways to anneal the sample; thermal annealing or solvent annealing. Thermal annealing consists of heating the substrate above the glass transition temperature of P3HT which allows the polymer chains to reorganize and allows the

www.manaraa.com

PCBM molecules to freely diffuse into the composite and reorder in a more thermodynamically favorable way. Solvent annealing consists of controlled or slow evaporation of the solvent from the active layer as opposed to fast drying. Fast drying (few seconds) happens naturally for solvents such as chloroform that evaporate quickly due to their high boiling point. Fast drying of the solvent for high boiling point solvents like dichlorobenzene would require the assistance of nitrogen, which naturally dries in several minutes. The presence of solvent molecules during drying allows the film to naturally phase separate [12]. The results of thermal and solvent annealing are approximately the same and the primary consequences of either method are more highly ordered polymer chains which both increases the absorption spectrum and absorption coefficient of the film [4].

Although the P3HT/PCBM system has been successful in reaching efficiencies above 5%; when looking at this system closely, it can be seen that several improvements can be made. The minimum energy necessary to ensure exciton splitting and charge dissociation is a difference of 0.3eV in LUMO levels of the acceptor and donor. As can be calculated from the band diagram shown in Figure 5, this difference in the P3HT/PCBM system is 1eV. The bandgap of P3HT is higher than the ideal bandgap for a polymer absorber of about 1.5eV [4].

www.manaraa.com

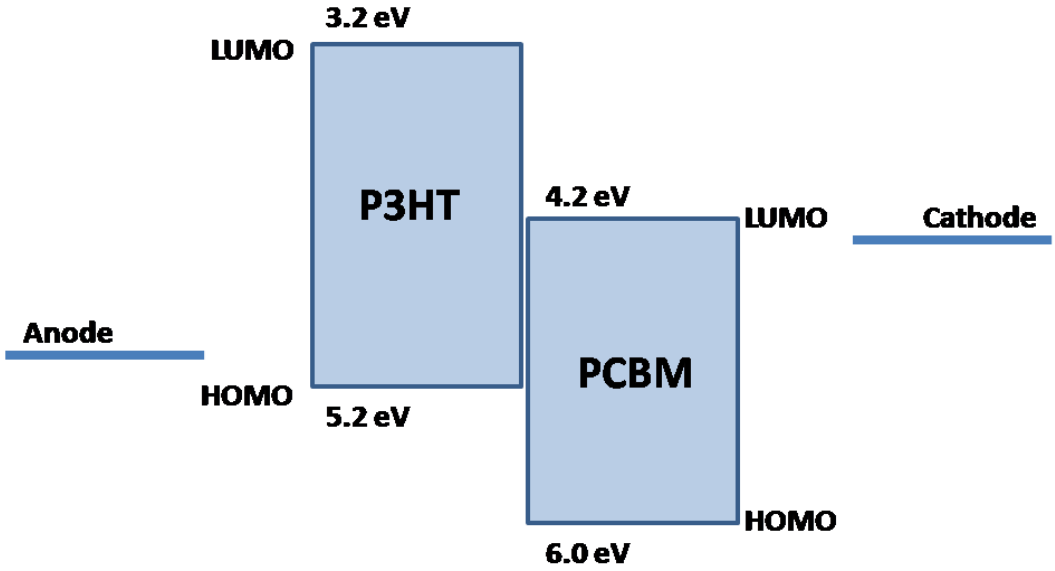

Figure 5: Energy band diagram for P3HT/PCBM system. All values are relative to the vacuum level.

To decrease the difference between the HOMO levels of the materials, a donor with a higher electron affinity or an acceptor with a lower electron affinity would need to be fabricated. At the same time the difference between the HOMO of the donor and LUMO of the acceptor should be kept as large as possible to have a high open circuit voltage.

The solubility of C_{60} is limited with PCBM being the most common soluble form, although other soluble forms exist including pEHO-PCBM and p-EHO-PCBA, shown in Figure 6. The HOMO levels are approximately the same as PCBM; however, the bandgaps are slightly larger, resulting in an increase in the open circuit voltage of devices made with them. However, the short circuit current was lower [11].

www.manaraa.com

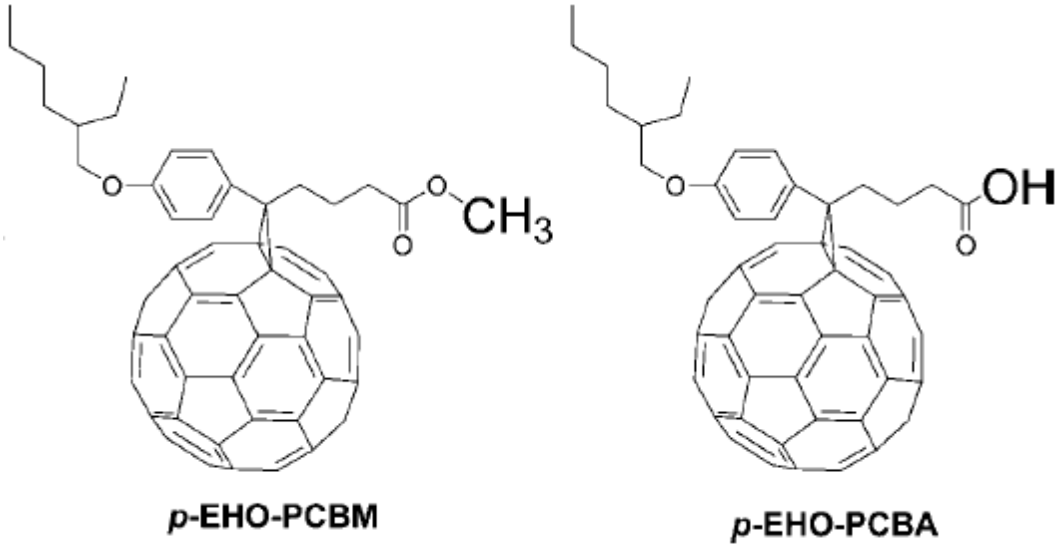

Figure 6: Soluble C_{60} derivatives other than PCBM [11].

Polymers, in comparison are relatively easy to manipulate and synthesize and are naturally soluble. For this reason much effort has been made to create new materials with better intrinsic properties than P3HT. New materials that can replace P3HT should have a higher electron affinity, a lower band gap, or both. Other things to consider include the solubility of the polymer, its miscibility with PCBM, its hole mobility, the solvent used, processing conditions, and the morphology of the finished film, as these have all been shown to have drastic effects on device performance.

The largest power conversion efficiency reported for organic solar cells is are made from a series of semiconducting polymers based on alternating ester substituted thieno[3,4-b]thiophene and benzodithiophene (PTB) units [13]. These polymers exhibit a combination of properties that lead to an excellent photovoltaic effect. The polymers have a low bandgap of about 1.6eV and show efficient absorption within the solar spectrum. The rigid backbone

www.manaraa.com

results in a good hole mobility of the polymer and also show good solubility in organic solution and suitable miscibility with the fullerene acceptor. The relatively low-lying HOMO energy level offers an enhanced Voc. The stacking of the polymer chains is of a different arrangement than P3HT and has been shown to be advantageous for charge transport. All these advantages make PTBs good candidates for BHJ polymer/fullerene solar cell applications and power conversion efficiencies up to 6.1% has been achieved from PTB4/$PC_{61}BM$ prototype devices.

Devices made from PTB7/$PC_{71}BM$ have shown power conversion efficiencies as high as 7.4%. PTB7 shows strong absorption from 550nm to 750nm; however, the combination of PTB7/$PC_{71}BM$ shows strong absorption throughout the visible spectrum from 300nm to 750nm. This is because $PC_{71}BM$ provides absorption in that lower range. The hole mobility was shown to be $5.8x10^{-4}cm^2/Vs$ which exceeds both the desired minimum of $10^{-4}cm^2/Vs$ for obtaining efficient geminate separation and the hole mobility of P3HT. The optimized cell had an active layer thickness of 100nm, a weight ratio of 1:1.5, and a mixed solvent of 3% diiodoctane in dichlorobenzene. The resulting short circuit current and open circuit voltage was $14.5mA/cm^2$ and 0.75V; respectively, with a fill factor of 69%. In addition, both the internal and external quantum efficiencies were very high implying that the harvest of solar energy was efficient.

1.4 Objective of this dissertation

The primary objective of study performed under this dissertation is to characterize, evaluate, and optimize the photovoltaic performance of a new class of conjugated polymers synthesized by Malika Jeffries-El group (Chemistry Department, Iowa State University).

www.manaraa.com

These two new polymers are poly (3,4-didodecylthiopene vinylene)-2,6-diyl benzo [1,2-d; 5,4-d'] bisoxazole] (cis-DD-PTVBBO) and poly (3,4-didodecylthiopene vinylene)-2,6-diyl benzo [1,2-d; 4,5-d'] bisoxazole] (trans-DD-PTVBBO). Electron affinities were measured be 3.02eV for cis-DD-PTVBBO and 3.10eV for trans-DD-PTVBBO. The optical bandgaps are around 2eV for both polymers. The low band gap and high electron affinity of these polymers suggest that they would be suitable candidates for use in bulk heterojunction solar cells with PCBM. Solar cells using the cis-DD-PTVBBO and the trans-DD-PTVBBO as the electron donor were fabricated and device characteristics were measured. In addition, hole mobilities were measured and atomic force microscopy (AFM) characterization was performed to evaluate phase separation in the thin films of the active layers.

www.manaraa.com

Chapter 2: Sample preparation

2.1 Polymer synthesis

Fully conjugated rigid-rod polybenzobisoxazoles (PBO)s are multifunctional materials widely known for their excellent tensile strength and thermal stability [14]. PBOs also have many beneficial properties for use in organic semiconducting applications including efficient electron transport [15], photoluminescence [16], and high electron affinity [17]. In spite of these qualities the development of PBOs has faltered since the initial research on their optical and electronic properties. This is largely due to their poor solubility, which requires PBOs to be processed from acidic solutions; and the harsh reaction conditions for their synthesis, which limits the types of substituents that can be incorporated onto the polymer backbone. To realize the untapped potential of the benzobisoxazole moiety for the development of novel conjugated polymers, an alternative approach was developed toward benzobisoxazole synthesis using mild conditions [18]. As a result 2,6-difunctionalized benzobisoxazoles have been prepared which can be used as monomers for the synthesis of soluble PBOs by appending flexible side-chains onto the aryl co-monomers.

Two new PBOs were synthesized, namely poly (3,4-didodecylthiopene vinylene)-2,6-diyl benzo [1,2-d; 5,4-d'] bisoxazole] (cis-DD-PTVBBO) and poly (3,4-didodecylthiopene vinylene)-2,6-diyl benzo [1,2-d; 4,5-d'] bisoxazole] (trans-DD-PTVBBO). The unique combination of the benzobisoxazole, thiophene, and vinylene moieties greatly enhances the properties of the resultant polymer by: 1) using the internal charge transport between the electron accepting benzobisoxazole and electron donating thiophene rings to reduce the band gap; 2) incorporating vinylene linkages to reduce steric interactions between

www.manaraa.com

consecutive aromatic rings, further reducing the band gap; 3) increasing rotational freedom of the polymer backbone increasing solubility; and 4) reducing the π-π interactions by adding the alkyl side chains greatly improving the solubility of polymer.

The synthesis of cis-DD-PTVBBO and trans-DD-PTVBBO, shown in Figure 7, was accomplished by the Horner-Wadsworth-Emmons polycondensation between 3,4-didodecyl-2,5-thiophenedicarboxaldehyde and a benzobisoxazole monomer. The robust benzobisoxazole moiety was stable to the basic reaction conditions. The resulting polymers were highly soluble in standard organic solvents, such as tetrahydrofuran (THF) and chloroform at room temperature facilitating the formation of optical quality thin films. The relative molecular weight obtained for cis-DD-PTVBBO was M_w=13,400 with a polydispersity index (PDI) of 2.38 and trans-DD-PTVBBO had M_w =10,800 with a PDI of 2.68. Thermogravimetric analysis revealed that both polymers were thermally stable with 5% weight loss onsets occurring only around 300°C under air. Additionally, differential scanning calorimetry (DSC) revealed weak glass transition temperature of 106°C for cis-DD-PTVBBO, whereas trans-DD-PTVBBO did not show any observable transitions before their decomposition temperature.

www.manaraa.com

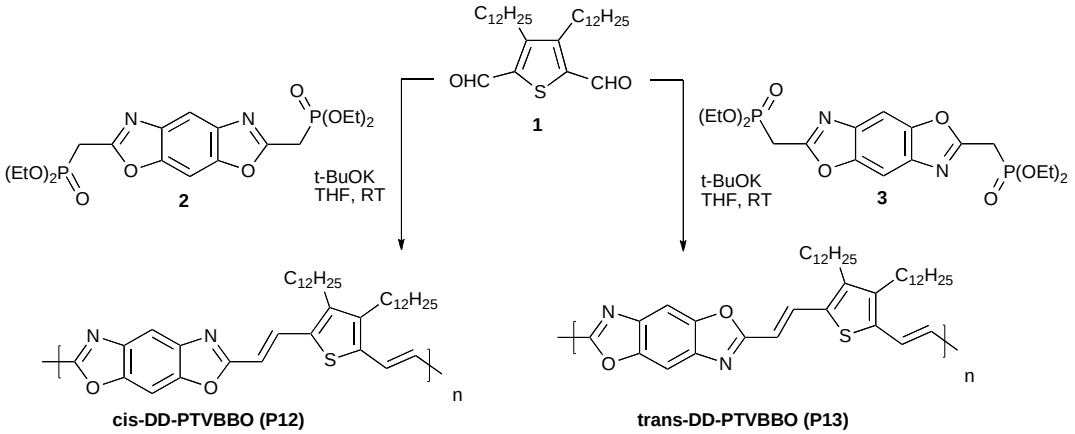

Figure 7: Synthesys of cis-DD-PTVBBO and trans-DD-PTVBBO.

The photophysical characteristics of the polymers were evaluated by UV-vis absorption and fluorescence spectroscopy both as dilute solutions in THF and thin films. In solution, the UV spectra of both polymers have a single broad absorbance bands, whereas the thin film absorbance spectra for both polymers are slightly broader. The absorption maximum for trans-DD-PTVBBO was red-shifted to 27nm relative to the absorbance maximum for cis-DD-PTVBBO. The optical band gaps for the polymers were estimated from absorption onsets to be 2.04ev for cis-DD-PTVBBO and 2.17eV for trans-DD-PTVBBO. The normalized absorbance and emission spectra for the polymers in solutions and thin films are shown in Figure 8 and Figure 9.

www.manaraa.com

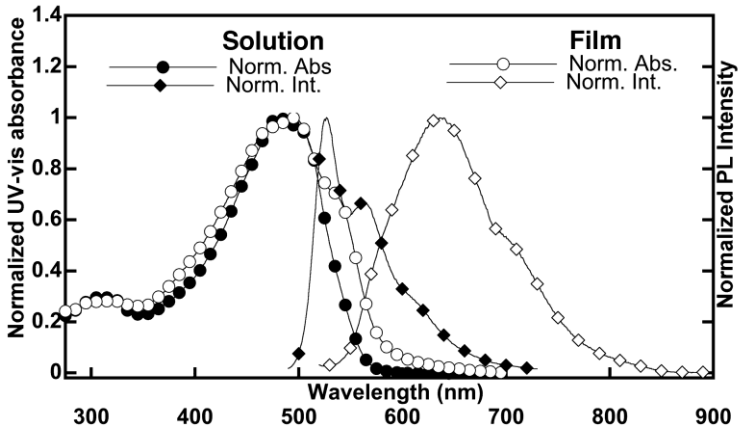

Figure 8: Absorption and emission spectrum for cis-DD-PTVBBO.

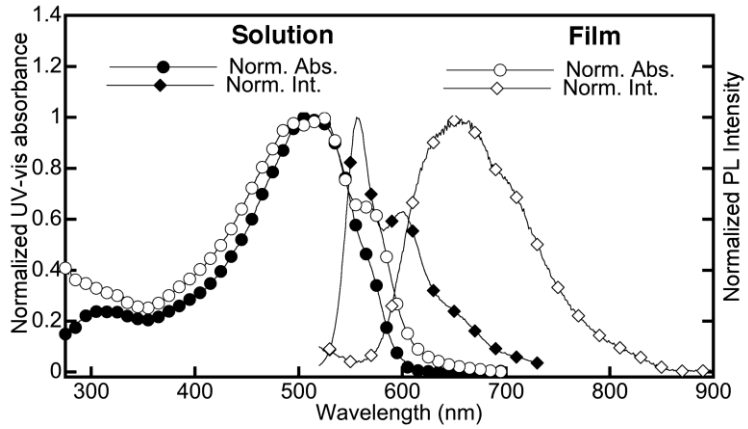

Figure 9: Absorption and emission spectrum for trans-DD-PTVBBO.

In solution both the photoluminescence spectra of both polymers have two excitations. As with the UV spectra the emission spectra of the trans-PTVBBO is red-shifted relative to the cis-PTVBBO. As films, the emission spectra of the polymer thin films were considerably red-shifted, relative to corresponding solution spectra. This phenomenon is most likely caused by aggregation and excimer formation. When the polymers were mixed

www.manaraa.com

with PCBM, the fluorescence was quenched, suggesting efficient charge transfer between the two materials.

The electrochemical properties of the polymers were investigated by cyclic voltammetry (CV). The data was obtained from polymer thin films on a platinum working electrode, in acetonitrile, using 0.1 M $(Bu)_4NPF_6$ as the electrolyte and an Ag/Ag^+ (0.01 M $AgNO_3$ in acetonitrile) reference electrode. The onsets were referenced to Fc/Fc^+. Both polymers exhibited fully reversible reduction waves, whereas oxidation waves were not observed for either polymer. Taking -4.8eV as the ferrocene energy level relative to vacuum, it was estimated that the LUMO levels for the polymers to be -3.02 for cis-DD-PTVBBO and -3.10 eV for trans-DD-PTVBBO, relative to vacuum. Since oxidation onsets could not be measured for the polymers, the HOMO values were calculated using the optical band gaps and the LUMO levels.

2.2 Device fabrication

Because organic solutions are sensitive to both light and oxygen, all solutions were made inside of a glovebox with argon atmosphere. The solutions were kept from exposure to light by covering the solution bottles with aluminum foil. Powders of the desired polymer and PCBM were measured and placed in clean glass vials in which a stir bar had already been placed. The solvent was then measured using a pipette and placed in the vial. All solutions had a combined polymer and fullerene concentration of 20mg/mL of solvent. The solution was then placed on a hotplate at 40°C and stirred overnight to ensure complete dissolution of the phases.

www.manaraa.com

Clean indium tin oxide (ITO) covered glass slides were prepared by placing them in a series of solutions and sonicating the solutions for ten minutes each. The solutions consisted of acetone, isopropyl alcohol, detergent, and deionized (DI) water. The slides were rinsed in DI water after each solution before being placed in the next in an effort to minimize contamination of the solutions. The slides were then dried with nitrogen. Finally, the slides were placed in a plasma cleaner ITO side up. The surface of the ITO slides was bombarded with charged ions of an oxygen plasma which easily breaks down any organic contaminates. The charged ions bombarding the surface also cause the surface to become hydrophilic which will promote the adhesion of a Poly(3,4-ethylenedioxythiophene) poly(styrenesulfonate) (PEDOT:PSS) layer as PEDOT:PSS is also a hydrophilic solution.

PEDOT:PSS was then spin coated at 3000rpm for 100sec onto the ITO slides under a fume hood to prevent contamination of the newly cleaned slides. This resulted in a 50nm PEDOT:PSS layer. The PEDOT:PSS was first filtered using a 0.45um filter to ensure that no particles larger than the layer thickness are present. The PEDOT:PSS serves two purposes. First, it is a hole conducting layer with a high work function to help promote hole collection in the ITO contact. Second, it helps smooth out the rough surface of the ITO reducing the probability of fabricating a device with shorts. Because PEDOT:PSS is in an aqueous solution, the slides were placed on a hotplate for five minutes at 120°C to ensure complete evaporation of the water before transfer into the glovebox. The glovebox, in addition to being oxygen free, is also moisture free.

The slides were then transferred into the glovebox with argon atmosphere where the active layer would be spin coated. After filtering the solutions through a 0.45um filter, the

www.manaraa.com

polymer and PCBM mixture was spin coated at 600rpm for 60sec, resulting in an approximately 200nm thick active layer. The samples were left in the glove box to solvent anneal for at least two hours before aluminum contacts were thermally evaporated. Solvent annealing is a method of allowing the solvent to evaporate without the aid of additional heat. This method of annealing has been found to produce highly organized films in the P3HT/PCBM system [12]. During the annealing process the samples were covered with aluminum foil to prevent exposure to light. Once the samples had annealed, exposure to oxygen and light is less of an issue as the reaction rate slows down significantly when not in solution. Knowing this, the samples were transferred out of the glove box and aluminum contacts were thermally evaporated resulting in an approximately 100nm thick top contact.

www.manaraa.com

Chapter 3: Characterization methods

3.1 Current-voltage (IV) curves

The IV curve is a simple measurement from which several important parameters of a solar cell can be determined including the short circuit current or current density (I_{sc} or J_{sc}), the open circuit voltage (V_{oc}) and the fill factor (FF). The FF is determined according to the following formula

$$FF = \frac{V_m J_m}{V_{oc} J_{oc}}$$

where J_m and V_m represent the current density and the voltage; respectively, at the maximum output power point. The concept can be seen more clearly in Figure 10.

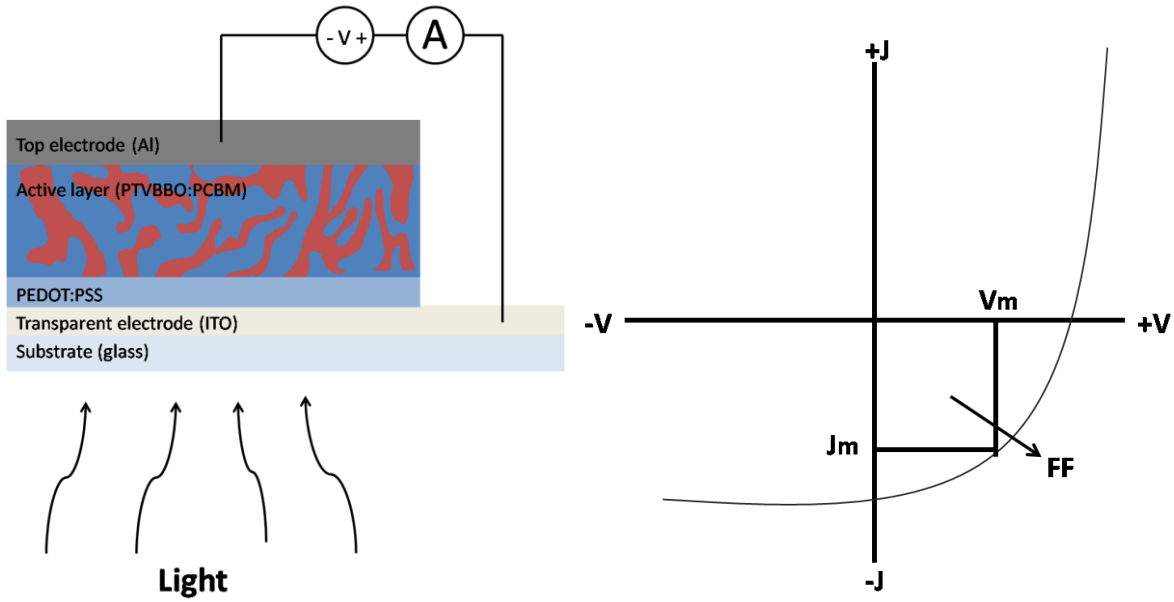

Figure 10: Current-Voltage measurement.

The IV curves taken on our devices were done at room temperature under ambient air conditions under the illumination of an ELH bulb. The polymer on a corner of the substrate

www.manaraa.com

was carefully removed to expose the ITO so that an electrical contact could be made. The other probe was connected to the top contact and the applied voltage was swept while the resulting current was measured. The IV curve was plotted, the J_{sc} and V_{oc} was taken note of, and the FF was calculated.

3.2 Hole mobility using space charged limited current (SCLC)

Hole only devices were fabricated in the same manner as explained in section 3.1 except that gold was used as the top contact instead of aluminum. The work function of gold (5.2eV) is such that the fabricated devices would be primarily hole conducting devices. This is sometimes referred to as 1-dimensional devices of measurement, indicating that carrier movement only occurs in one direction. The mobility of the holes was then measured using the space charge limited current (SCLC) method. SCLC occurs when the charges injected from an ohmic contact exceed the resident majority charge density. Numerically, this happens when

$$\varepsilon * E_{applied} = \frac{qp_0L}{A}$$

where $\varepsilon = \varepsilon_o\varepsilon_r$ is the permittivity of the material, $E_{applied}$ is the applied electric field, q is the charge of an electron (1.6×10^{-19} C), p_o is the resident majority carrier concentration, L is the thickness of the sample, and A is the area of the contact.

The IV curve of a semiconductor device has three distinct regions. With low electric field, the current follows the applied voltage in a linear fashion in accordance with Ohm's law; Voltage = Current*Resistance. However; at higher electric fields, current increases as the voltage squared and Ohm's law is no longer valid. The third region of the IV curve is

www.manaraa.com

saturation. In this region, the current does not increase with voltage due to the increased average velocity of the majority carriers. This velocity causes collisions to occur much more often and impedes the motion of carriers in response to the applied electric field.

To determine the majority carrier concentration present in the sample, the IV curves were analyzed to determine the point of transition between the linear and V^2 regions, commonly called V_{sclc}. The magnitude of this voltage is directly related to the mobility through the following equation

$$\mu = \frac{8L^3 J}{9\varepsilon V^2}.$$

3.3 Quantum efficiency

Quantum efficiency is defined as the number of electrons collected divided by the number of photons input. A diagram of the QE setup is shown in Figure 11.

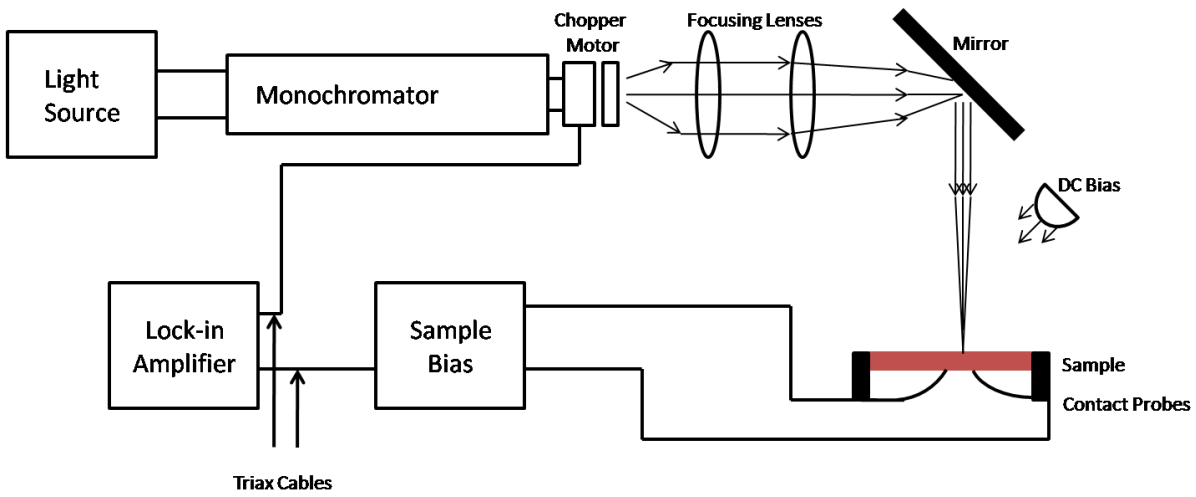

Figure 11: Schematic diagram for quantum efficiency measurements.

The samples are measured using a dual beam setup. A DC light is used to ensure that the carrier lifetimes remain nearly constant. A monochromatic light is then shined on the sample

www.manaraa.com

to measure the photoconductivity of the sample. By passing the monochromatic light beam through a chopper motor at a frequency of 13 Hz, a lock-in amplifier can be used to measure signals with very low signal to noise ratios. The frequency of 13Hz is chosen because it is not a multiple of 60Hz which is the frequency of room lights; and this helps reduce noise. The range of wavelengths measured was from 400-900 nm, as this is the range of wavelengths that the device is the most active and corresponds to the solar spectrum. During this scan, the device is measured at both a 0 V bias and a -0.5 V bias. The measurement under negative bias can give information about the electric field in the device and carrier transport. For example, if large barriers exist within the device, the QE of the 0V and -0.5V bias will vary greatly, while the absence of barriers would result in almost identical curves. Knowing at which wavelengths any differences occur can also be correlated to where in the device the barriers exist. This is because different wavelengths will be absorbed at different places within the device. A normalized QE measurement is generally used for our devices where they are normalized at the peak value which is set to 0.90 or 90%. To determine the actual QE of the device a reference cell with a known QE and area is used where

$$QE_{sample} = QE_{ref}\left(\frac{A_{ref}V_{sample}}{V_{ref}A_{sample}}\right)$$ [19].

3.4 Atomic force microscopy

The Atomic Force Microscope (AFM) is an instrument that can analyze and characterize samples at the microscope level. This means we can look at surface characteristics with very accurate resolution ranging from 100μm to less than 1μm.

www.manaraa.com

The AFM operates by allowing an extremely fine sharp tip to either come in contact or in very close proximity to the sample that is being imaged. This tip is usually a couple of microns long and often less than 100Å in diameter. The tip is located at the free end of a cantilever that is 100 to 200μm long. The sample is then scanned beneath the tip. Different forces either attract or repeal the tip (Figure 12). These deflections are recorded and processed using imaging software; the resulting image is a topographical representation of the sample that was just imaged. The force is not measured directly, but calculated by measuring the deflection of the lever, and knowing the stiffness of the cantilever. Hook's law gives F = -kz, where F is the force, k is the stiffness of the lever, and z is the distance the lever is bent.

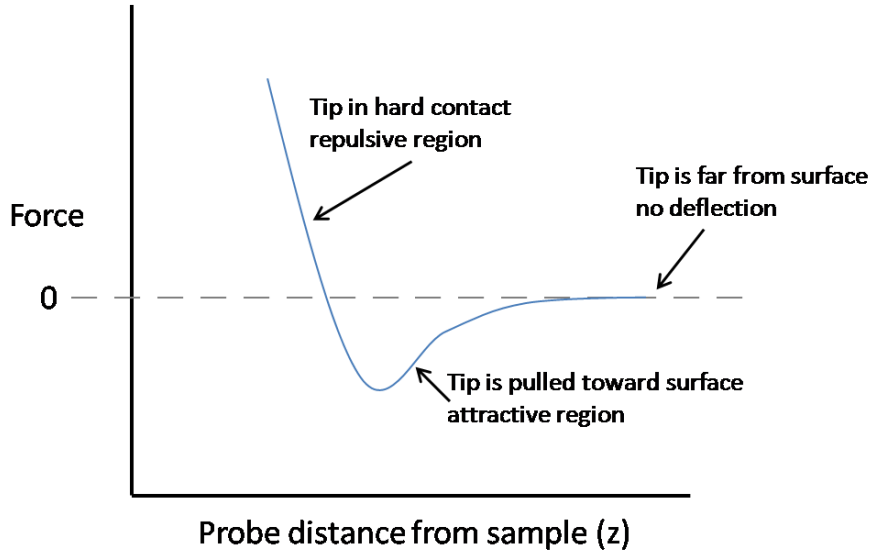

Figure 12: Force vs sample distance for different methods of measurement.

www.manaraa.com

In the contact region, the cantilever is held less than a few angstroms (10^{-10}m) from the sample surface, and the interatomic force between the cantilever and the sample is repulsive. In the non-contact region, the cantilever is held on the order of tens to hundreds of angstroms from the sample surface, and the interatomic force between the cantilever and sample is attractive. Different scanning modes operate in different regions of this curve: Non–contact in the attractive region, contact mode in the repulsive and intermittent or tapping mode fluctuates between the two [20].

Tapping mode can be easily used in conjunction with other modes such as force modulation and phase imaging. Force modulation refers to a method used to probe properties of materials through sample/tip interactions. The tip (or sample) is oscillated at a high frequency and pushed into the repulsive regime. The slope of the force-distance curve is measured which is correlated to the sample's elasticity. In Phase mode imaging, the phase shift of the oscillating cantilever relative to the driving signal is measured. This phase shift can be correlated with specific material properties that effect the tip/sample interaction. The phase shift can be used to differentiate areas on a sample with such differing properties as friction, adhesion, and viscoelasticity [21].

Our samples were measured using tapping mode and topography and phase images were obtained and analyzed. Our primary interest was the phase separation of the film, as it should be on the same order of magnitude as the exciton diffusion length for efficient exciton dissociation.

www.manaraa.com

Chapter 4: Results

4.1 Photovoltaic characterization

At the outset, we were interested to evaluate which of the two polymer versions, cis-PTVBBO or trans-PTVBBO, has better photovoltaic performance. Therefore; two solutions of a 1:1 ratio of polymer to fullerene were created with an overall resulting concentration being 20mg of polymer and fullerene per mL of solvent. The solvent used in this case was ortho-diclorobenzene (o-DCB). The active layer was spin coated on a PEDOT:PSS coated ITO glass substrate. Aluminum cathodes were then evaporated; after which current voltage measurements were conducted. The IV curves for these devices are shown in Figure 13. It can be seen that the trans-PTVBBO based cells performed much better with a higher short-circuit current (0.66 mA/cm2) than cis-PTVBBO based devices (0.12 mA/cm2). The fill factor of trans-PTVBBO cells (31%) was also higher than cis-PTVBBO cells (26%). The open circuit voltages were comparable, between 0.35 V and 4V; however, lower than would be expected based on the band diagram for the system. This is not surprising as it has been shown by several research groups that open circuit voltage can deviate from the theoretical maximum if other aspects of the device are imperfect. These other aspects can be a non-ohmic contact at the polymer electrode interface, impurities within the polymers, or non-optimum phase separation in both vertical and horizontal directions upon spin coating of the active layer. The superior performance of photovoltaic cells based on trans-PTVBBO in comparison to cis-PTVBBO can be attributed to higher electron affinity and smaller bandgap of the trans-PTVBBO.

www.manaraa.com

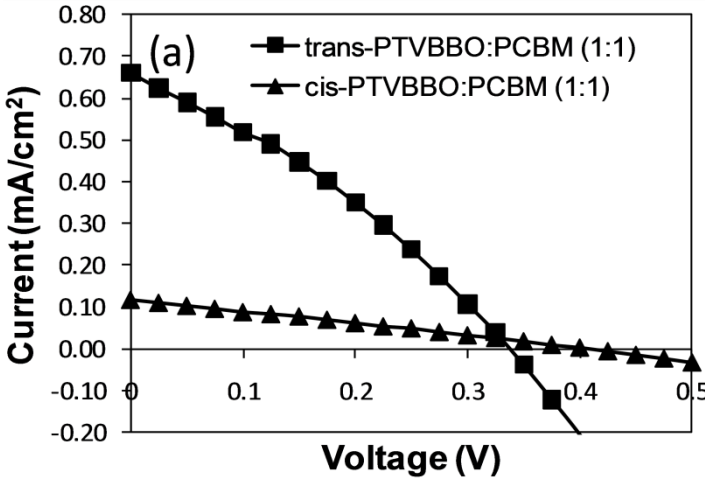

Figure 13: JV curve for 1:1 polymer:PCBM ratio devices.

While the performance of the trans-PTVBBO devices is lower than other state of the art conjugated polymers, it should be noted that these PV cells are the first to be fabricated from copolymers containing benzobisoxazoles and thiophene. As a result, many processing parameters such as choice of solvent (or solvent mixtures), annealing conditions, and polymer/PCBM ratios are not yet optimized. All of these parameters are critical, and their optimization alone has led to drastic improvements in power conversion efficiencies of photovoltaic cells based on other conjugated polymers such as rr-P3HT and poly[N-9′-heptadecanyl-2,7- carbazole-alt-5,5-(4′,7′-di-2-thienyl-2′,1′,3′-benzothiadiazole)] (PCDTBT). In part, the poor performance of the PVCs fabricated in this report can be ascribed to a non-optimal phase separation, as shown in the atomic force microscopy AFM phase image (Figure 14). Aggregates of size 50-100 nm are observed, which are much larger than typical exciton diffusion lengths of conjugated polymers (~10 nm). Although we could dissolve PTVBBO in DCB, this solution does not pass though the 0.45 micron filter as readily as solutions of rr-P3HT in DCB. This suggests that there are large aggregates of polymers in the solution. Thus, improving the dissolution of these benzobisoxazole polymers in higher

www.manaraa.com

boiling point solvents in expected to result in improved performance. It should be noted that we mention high-boiling point solvent here because they seem to be most promising for high efficiency solar cells. They dry much slower than low boiling point solvents and this allows the polymer to slowly self-assemble into a more crystalline form. Higher crystallinity is important for better charge transport.

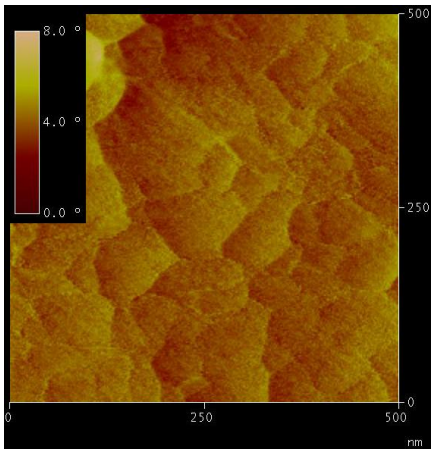

Figure 14: AFM phase image of trans-DD-PTVBBO thin film. Scan Size: 500 nm by 500nm.

As a natural next step, we decided to investigate the effect of changing PCBM concentration on the performance of our PV cells. Different polymers have different ideal polymer:fullerene ratios. For example, a P3HT:PCBM ratio of 1:1 is the best for photovoltaic devices; however, MDMO-PPV optimizes at a polymer:fullerene ratio of 1:4 [22]. This is because if there is enough free space between polymer side-chains to accommodate more than one fullerene molecule, then more than 1 fullerene will be needed per polymer chain for efficient exciton dissociation process.

www.manaraa.com

To investigate whether such an effect is valid for PTVBBO, we fabricated photovoltaic devices with 1:1, 1:2, 1:3, and 1:4, of polymer:fullerene ratio for both cis and trans versions. Table 1 shows the photovoltaic parameters for these devices. As can be seen, trans-PTVBBO devices again performed better than the cis-PTVBBO devices as they had higher short circuit currents, comparable open circuit voltages, and higher fill factors. For cis-PTVBBO, short-circuit current and open circuit voltage increased for increasing fullerene content, indicating towards fullerene intercalation between polymer side-chains for higher polymer-fullerene ratios. Fill factor; however, first decreases and then increases as fullerene amount is increased; the reason of which is not clear at this point. The trend was different for trans-PTVBBO. As can be seen from Table 1 and Figure 15, the short-circuit current, open-circuit voltage, and fill-factor all seem to become better for 1:2 and 1:3 polymer:fullerene ratios, but then worsens for the 1:4 ratio. The highest short-circuit current was achieved for 1:2 polymer:fullerene ratio, whereas highest open-circuit voltage and fill-factor was achieved for 1:3 polymer:fullerene ratio.

Table 1: JV curve measurement results for all ratios

	Jsc (mA/cm^2)		Voc (V)		FF	
Cis-TVBBO	Avg	Max	Avg	Max	Avg	Max
1:1	0.072	0.096	0.423	0.436	25.47	26.54
1:2	0.183	0.231	0.495	0.508	22.80	23.64
1:3	0.239	0.263	0.594	0.597	20.07	20.17
1:4	0.318	0.342	0.583	0.599	24.31	25.05
Trans-TVBBO						
1:1	0.828	0.883	0.309	0.393	30.76	31.86
1:2	0.977	1.011	0.432	0.449	34.74	35.44
1:3	0.865	0.955	0.399	0.464	34.77	37.65
1:4	0.831	0.908	0.259	0.312	30.97	33.01

www.manaraa.com

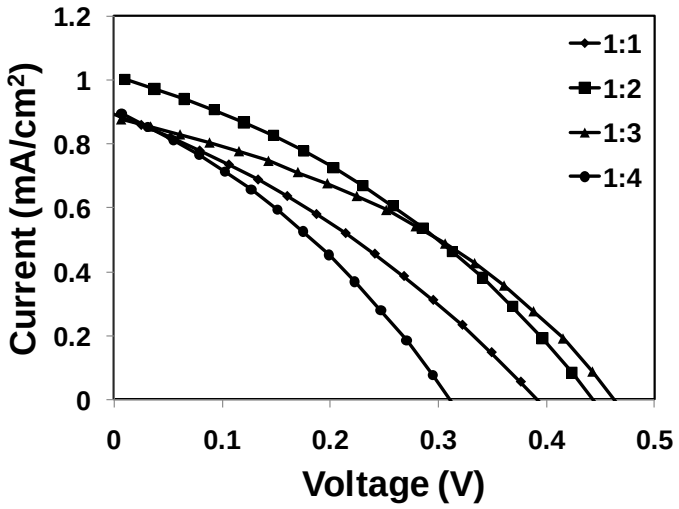

Figure 15: JV curves for trans-DD-PTVBBO:PCBM using diclorobenzen as the solvent.

Solubility was a major concern for this polymer so different solvents were tested for solubility. To evaluate the device-relevant quality of solvent, hole mobility was also measured in polymer thin films casted from these solvents. Tetrahydofuran (THF) was the only solvent that could be filtered using only human strength. All other solvents required the solution to be passed through a filter at very high pressures. As we will see in section 4.3, trans-DD-PTVBBO thin film spin coated from ortho-dichlorbenzene possessed the highest hole mobility ($3.8x10^{-5}cm^2/Vs$) compared to the other solvents. Because trans-PTVBBO were the most soluble in THF, devices with a 9:1 mixture of THF and o-DCB were also created which resulted in a higher open circuit voltage (~0.6V); however, an even lower short circuit current (~$0.15mA/cm^2$) and a low fill factor (~22%). Annealing conditions have been shown to have a large influence on the performance of solar cells as it allows the polymer chains to align in a more ordered pattern. Solvent annealing was the method used in this

www.manaraa.com

study, but it is likely that the THF solvent dries too quickly for the polymer chains to align. Thermal annealing of devices made with THF may have resulted in better performance, and is a recommended future direction.

4.3 Hole mobility using space charged limited current (SCLC) model

Photovoltaic characterization indicated that trans-DD-PTVBBO appears to have more potential than the cis version. Thus we only focused on the trans version for the mobility studies. The goal of characterizing the hole mobility was two-fold: 1) to determine the best solvent for charge transport; and 2) to probe whether blending with fullerenes increases the mobility or not. Trans-DD-PTVBBO was spin coated from four different solvents and hole-only diodes were created by evaporating gold contacts. I-V characteristics were then evaluated using the SCLC model. Chloroform, dichlorobenzene, toluene, and chlorobenzene were the different solvents chosen. THF was also planned to be tested; however, due to the low boiling point of THF, the films dried almost immediately creating films that were too poor to create devices from. This would also explain why the I_{sc} of the devices made from the mixture of THF and o-DCB was so poor.

The IV characteristics of Figure 17 and table 2 shows that the hole mobility of trans-DD-PTVBBO thin film spin coated from dichlorobenzene solvent showed the highest hole mobility. The overall value of mobility ($3.8 \times 10^{-5} cm^2/Vs$) is comparable to the mobility values of other state-of-the-art conjugated polymers [23]. This shows that charge transport is not a reason for poor performance of our solar cells. Thus there is a stronger chance that poor solubility and presence of aggregates, as we hypothesized earlier, is a strong candidate behind the reason for poor PV performance. Mobility results show that such aggregates do

www.manaraa.com

not have a negative effect on the mobility measurements [24]. It is known that aggregates can transport charges well due to strong overlap between polymer chains.

Figure 18 show hole-only IV curves with different polymer:fullerene ratios. Solvent in this case was dichlorobenzene. The polymer:fullerene ratio of 1:1 showed the highest mobility; however, all other ratios showed similar mobilities. The difference in all mobilities is within one order of magnitude; therefore, we conclude that fullerenes have no effect on the hole mobility of trans-DD-PTVBBO, as it has in cases of some other conjugated polymers.

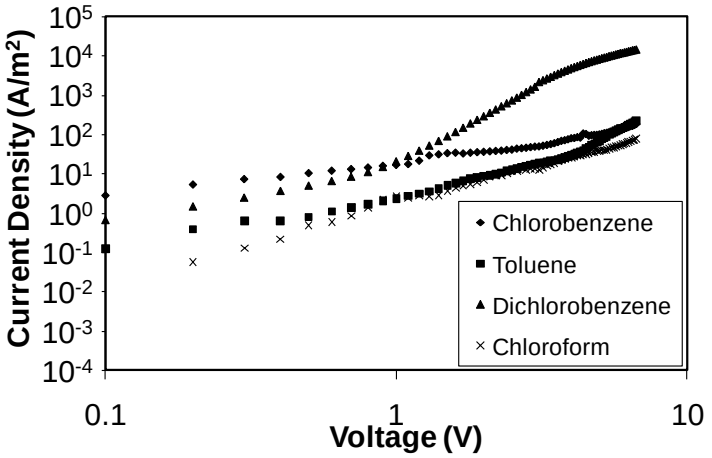

Figure 16: JV curves under SCLC to determine hole mobility using various solvents.

Table 2: The mobility of thin films of trans-DD-PTVBBO thin films derived from Figure 17 using the SCLC model.

Solvent	Mobility (cm^2/V-s)
Chlorobenzene	1.76E-05
Toluene	5.09E-06
Dichlorobenzene	3.80E-05
Chloroform	3.33E-06

www.manaraa.com

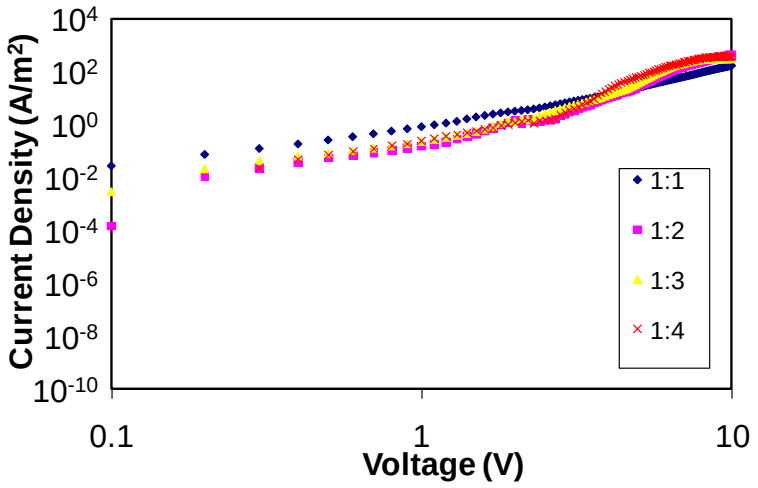

Figure 17: JV curves under SCLC for various ratios using dichlorobenzene as the solvent

4.4 Quantum efficiency

The normalized quantum efficiency (QE) for all ratios of the trans-PTVBBO devices are shown below in Figure 19. The QE at zero bias is less than the QE at 0.5V reverse bias indicating there are barriers within the device that affect the efficiency of charge collection. As the fullerene ratio in the blend is increased, the two curves begin to move closer together indicating that charge collection is becoming more efficient with increasing ratio; however, significant barriers still exist. For all ratios, the QE sees a sharp fall at 600nm because the polymer does not absorb any photons at wavelengths higher than 600 nm, due to its band gap being ~ 2eV. This is not the most optimal band gap because the solar spectrum is still very strong well past 600nm and these photons will not be collected. In the photovoltaic community, a band gap of approximately 1.4 eV is considered to be ideal for most optimum harnessing of solar spectrum. Current wavelength dependence of photocurrent does open up the possibility of using these cells in tandem architecture with lower band gap polymers.

www.manaraa.com

However, processing parameters would need to be optimized and overall performance would need to drastically increase before this option would be viable enough.

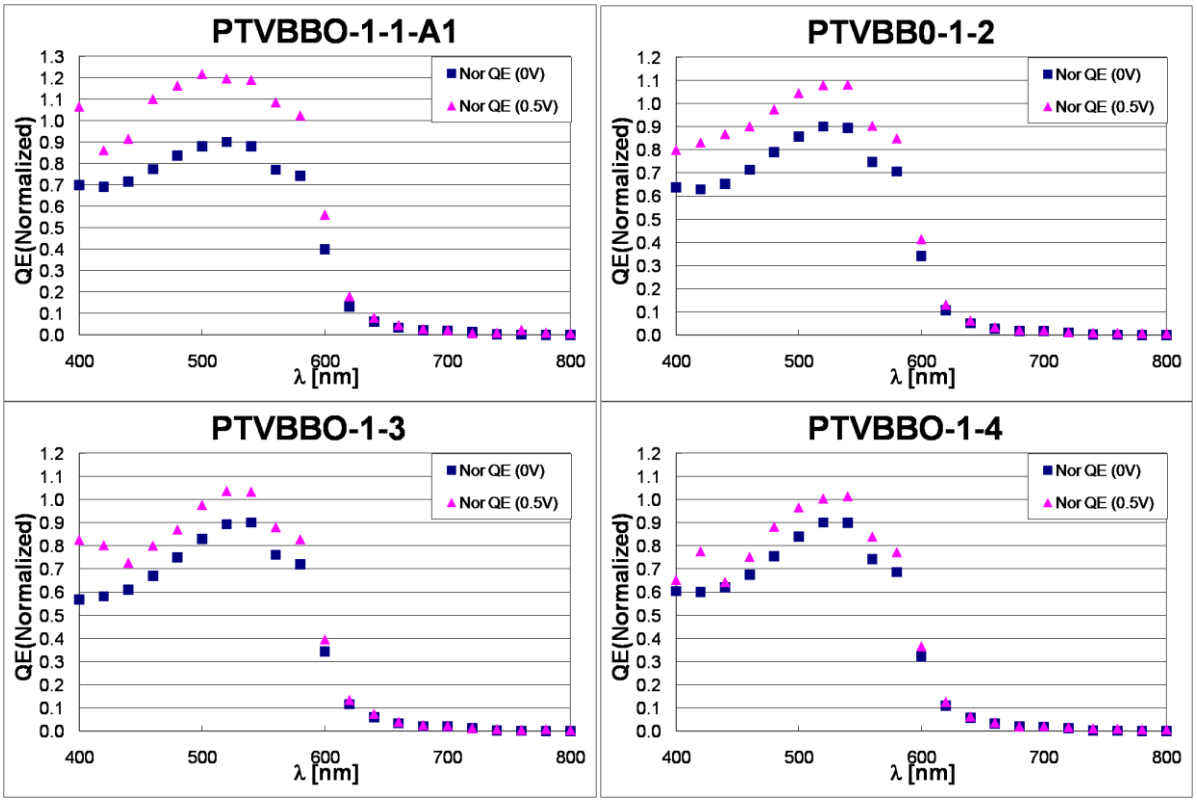

Figure 18: Normalized quantum efficiency of photovoltaic devices for different trans-DD-PTVBBO:PCBM ratios.

4.5 Atomic force microscopy

The nanoscale morphology of the trans-DD-PTVBBO:PCBM thin films were characterized using atomic force microscopy. Figure 20 shows the phase images of these thin films for all polymer:fullerene ratios. Ideally, the phase separation between the polymer and fullerene species should be on the order of the exciton diffusion length, which tends to be around 10nm. As can be seen in Figure 20, as the amount of fullerenes in the blend increases, the nanoscale intermixing or phase separation becomes better. For 1:1 ratio, the

www.manaraa.com

grain size is in the range of 50-100 nm, but for 1:3 and 1:4 ratios it appears to be less than 50 nm and closer to the ideal of 10nm. This in part explains why the 1:3 and 1:4 ratio devices performed better than the 1:1 ratio devices. However; it should be noted that the following AFM images are taken in good areas of the thin films. As was earlier mentioned, we faced solubility issues with this polymer. Hence, there will be other areas in the thin films where one can expect to see polymer aggregates. Those areas will have a limiting effect on the overall photovoltaic performance. This is why we believe that even 1:3 and 1:4 ratio devices perform much worse than the state-of-the-art P3HT:PCBM devices.

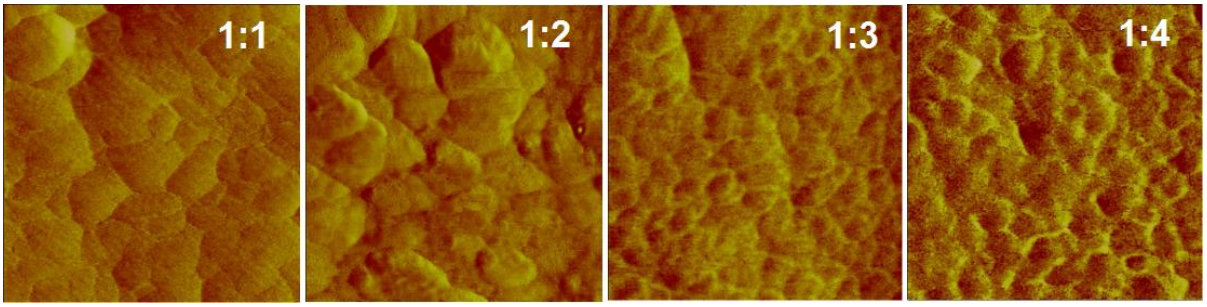

Figure 19: Phase measurements for different trans-DD-PTVBBO:PCBM ratios. 500nm x 500nm image. Phase separation increases with increasing ratio.

www.manaraa.com

Chapter 5: Conclusions and future work

It has been shown that two new polymers (cis-DD-PTVBBO and trans-DD-PTVBBO) from the polybenzobisoxazole (PBO) family can be synthesized without the traditional harsh acidic conditions required for their synthesys. Due to their ability to be disolved with organic solvents, the location of their electron affinity, their optical band gap, and the ability to transfer charge, photovoltaic devices were fabricated with these materials acting as the electron donor while PCBM was the electron acceptor.

It was determined that trans-DD-PTVBBO was a better photovoltaic material due to the higher currents and fill factors produced from these cells over the cis version. It was found that the phase separation of the trans-DD-PTVBBO and PCBM generally increased with an increasing polymer:fullerene ratio; however, even the smallest phase separation was still larger than optimal. This is partly suspected to be why the performance of the trans-DD-PTVBBO cells is still very poor when compared with other state of the art polymers such as P3HT. It is thought that the main reason for the performance is due to the poor solubility of the polymer in high boiling point solvents, leading to large aggregates in the film and poor film quality. It may also be the case that the poor performance is due to internal charge transfer between the electron donating thiophene unit and electron accepting benzobisoxazole unit.

Much must be done to improve the performance of the cis-DD-PTVBBO or trans-DD-PTVBBO polymers if they are ever to be considered commercially viable. It is suggested that this be done at the chemical level to improve the solubility of these polymers in high boiling point solvents. This can be done by adjusting the side chains on the polymer

www.manaraa.com

which controls the solubility of polymers in different solvents. It must also be determined if charge is being lost due to internal charge transfer between the electron donating thiophene unit and electron accepting benzobisoxazole unit of the polymer. If this is the case, charge is not being transferred to the PCBM phase and current is lost. Again, adjusting the polymer the chemical level would be the best approach to eliminate this issue. Finally, it is suggested that optimal material concentrations and annealing conditions be found, as these have been shown to have a very large influence on the performance of organic solar cells using other materials. In this work, solvent annealing was used; but it is possible that thermal annealing would lead to better performance, especially if low boiling point solvents are to be used.

www.manaraa.com

Acknowledgments

I would like to thank Sumit Chaudhary for being my major professor, allowing me to work on this research project, financial support, and guidance during this project. I would like to thank Nathan Neihart and Phillip Jones for serving on my committee. I would like to thank Kanwar Nalwa, Dan Putnam, and Rakesh Mahadevapuram for their direct help on this project. Finally, I would like to thank all the professors, teaching assistants, and friends that have helped me achieve during my graduate studies at Iowa State; including, but certainly not limited to, Vikram Dalal, Randall Geiger, Gary Tuttle, Phil Reusswig, Mike Beckman, Brian Lewis, Josh Jordan, Colin VanDercreek, and Rezza Rahmani. Finally, I would thank the state of Iowa's Office of Energy Independence for funding this project through Iowa Power Fund.

www.manaraa.com

References

[1] Renewables: Global status report. (2009). http://www.ren21.net/pdf/RE_GSR_2009_Update.pdf

[2] Jenny Nelson. Organic photovoltaic films. *Materials Today* (2002), p. 20-27.

[3] Brendan O'Connor; Pipe, Kevin; Shtein, Max. Fiber based organic photovoltaic devices. *Applied Physics Letters*. **92** (2008) 193306.

[4] B.C. Thompson and J.M.J. Frechet. Organic photovoltaics — Polymer-fullerene composite solar cells. *Angew. Chem. Int. Ed.* **47** (2008), p. 58−77.

[5] A.C. Mayer; Scully, S.; Hardin, B.; Rowell, M.; McGehee, M. Polymer-based solar cells. *Materials Today* **10** (2007), p. 28-33.

[6] Rene A.J. Janssen; Hummelen, J.C.; Sariciftci, N.S. Polymer-fullerene bulk heterojunction solar cells. *MRS Bulletin* **30** (2005), p. 33-36.

[7] Johann Boucle; Snaith, H.; Greenham, N. Simple approach to hybrid polymer/porous metal oxide solar cells from solution-processed ZnO nanocrystals. *Journal of Physical Chemistry* **114** (2010), p. 3664-3674.

[8] Chiatzun Goh; Scully, S; McGehee, M. Effects of molecular interface modification in hybrid organic-inorganic photovoltaic cells. *Journal of Applied Physics* **11** (2007), 114503.

[9] Gopal K. Mor; Kim, S.; Paulose, M.; Varghese, O.; Shankar, K.; Basham, J.; Grimes, C. Visible to near-infrared light harvesting in TiO_2 nanotube array—P3HT based heterojunction solar cells. *Nano Letters* **9** (2009), p. 4250-4257.

www.manaraa.com

[10] Zhenan Bao; Dodabalapur, A.; Lovinger, J. Soluble and processable regioregular poly(3-hexylthiophene) for thin film field-effect transistor applications with high mobility. *Applied Physics Letters* **69** (1996), p. 4108-4110.

[11] Changduk Yang; Kim, J.; Cho, S.; Lee, J.; Heeger, A.; Wudl, F. Functionalized methanofullerenes used as n-type materials in bulk-heterojunction polymer solar cells and in field-effect transistors. *Journal of American Chemical Society* **130** (2008), p. 6444-6450.

[12] Gang Li; Yao, L.; Yang, H.; Shrotriya, V.; Yang, G.; Yang, Y. Solvent annealing effect in polymer solar cells based on poly(3-heylthiophene) and methanofullerenes. *Advanced Functional Materials* **17** (2007), p. 1636-1644.

[13] Yongye Liang; Xu, Z.; Xia, J.; Tsai, S.; Wu, Y.; Li, G.; Ray, C.; Yu, L. For the bright future—Bulk heterojunction polymer solar cells with power conversion efficiency of 7.4%. *Advanced Materials* **22** (2010), p. 1-4.

[14] (a) J. F. Wolfe and F. E. Arnold; Rigid-rod polymers. 1. synthesis and thermal properties of para-aromatic polymers with 2,6-benzobisoxazole units in the main chain. *Macromolecules*, 1981, **14**, p. 909-915. (b) J. F. Wolfe and F. E. Arnold; Rigid-rod polymers. 2. synthesis and thermal properties of para-aromatic polymers with 2,6-benzobisoxazole units in the main chain. *Macromolecules*, **14** (1981) p. 915-920.

[15] M. M. Alam and S. A. Jenekhe. Polybenzobisazoles are efficient electron transport materials for improving the performance and stability of polymer light-emitting diodes. *Chemistry of Materials* **14** (2002), p. 4775-4780.

www.manaraa.com

[16] Yan Chen; Wang, S.; Zhuang, Q; Li, X.; Wu,P.; Han, Z. *Macromolecules* **38** (2005), p. 9873-9876.

[17] L.S. Tan; Burkett, J.; Simko, S.; Alexander, M. New aromatic benzazole polymers, 3-synthesis of rigid-rod benzobisazole polymers with main-chain 2,2-bipyridine-5,5-diyl units. *Macromolecular Rapid Communications* **20** (1999), p. 16-20.

[18] Jared Mike; Makowski, A.; Jeffries, M. An efficient synthesis of 2,6-disubstituted benzobisoxazoles: New building blocks for organic semiconductors. *Organic Letters* **10** (2008), p. 4915-4918.

[19] Philip Ruesswig**.** Measurement of minority carrier lifetimes in nanocrystalline silicon devices using reverse-recovery transient method. Iowa State University (2008).

[20] Galloway Group. Atomic force microscopy: A guide to understanding and using the AFM. 2004.

[21] http://www.nanoscience.com/education/AFM.html

[22] A.C. Mayer; Toney, M.; Scully, S.; Rivnay, J.; Brabec, C.; Scharber, M.; Koppe, M.; Heeney, M.; McCulloch, I.; McGehee, M. Bimolecular crystals of fullerenes in conjugated polymers and the implications of molecular mixing for solar cells. *Advanced Functional Materials* **19** (2009) p. 1173 – 1179.

[23] P. W. M. Blom; Jong, M.; Vleggaar, J. Electron and hole transport in poly(p-phenylene venylene) devices. *Applied Physics Letters* **68** (1996), p. 3308-3310.

www.manaraa.com

[24] Thuc-Quyen Nguyen; Doan, V.; Schwartz, B. Conjugated polymer aggregates in solution: control of interchain interactions. *Journal of Chemical Physics* **110** (1999), p. 4068-4078.

www.manaraa.com